Nanoscale

RSC Publishing

PAPER

View Article Online
View Journal | View Issue

Cite this: *Nanoscale*, 2013, **5**, 10963

Nanostructured TiO_2 surfaces promote polarized activation of microglia, but not astrocytes, toward a proinflammatory profile

Silvia De Astis,†[abc] Irene Corradini,†[abc] Raffaella Morini,[bd] Simona Rodighiero,[a] Romana Tomasoni,[bd] Cristina Lenardi,[ae] Claudia Verderio,[df] Paolo Milani[ae] and Michela Matteoli*[bd]

Received 10th July 2013
Accepted 26th August 2013

DOI: 10.1039/c3nr03534d

www.rsc.org/nanoscale

Activation of glial cells, including astrocytes and microglia, has been implicated in the inflammatory responses underlying brain injury and neurodegenerative diseases including Alzheimer's and Parkinson's diseases. The classic activation state (M1) is characterized by high capacity to present antigens, high production of nitric oxide (NO) and reactive oxygen species (ROS) and proinflammatory cytokines. Classically activated cells act as potent effectors that drive the inflammatory response and may mediate detrimental effects on neural cells. The second phenotype (M2) is an alternative, apparently beneficial, activation state, more related to a fine tuning of inflammation, scavenging of debris, promotion of angiogenesis, tissue remodeling and repair. Specific environmental chemical signals are able to induce these different polarization states. We provide here evidence that nanostructured substrates are able, exclusively in virtue of their physical properties, to push microglia toward the proinflammatory activation phenotype, with an efficacy which reflects the graded nanoscale rugosity. The acquisition of a proinflammatory phenotype appears specific for microglia and not astrocytes, indicating that these two cell types, although sharing common innate immune responses, respond differently to external physical stimuli.

Introduction

Activation of glial cells, *i.e.* astrocytes and microglia, has been implicated in the inflammatory responses underlying brain injury and neurodegenerative diseases, including multiple sclerosis, Alzheimer's and Parkinson's diseases. Astrocytes and microglia are two distinct types of glial cells in the central nervous system, and, although they are clearly distinct in embryonic origin, morphology and functional properties, they share some properties of immune active and supportive cells.[1] Also, microglia and astrocytes have the ability to either secrete soluble mediators triggering neural repair and contributing to the creation of an environment conducive to regeneration or release of neurotoxic cytokines and reactive oxygen species that regulate immune cell entry into the central nervous system (CNS) and are deleterious to the CNS. Under resting conditions, microglia are highly ramified cells, with a cell body fairly motionless, and long branches constantly moving and surveying the surrounding brain parenchyma.[2–4] Like macrophages, microglia are able to react to tissue insults by a rapid differentiation process, consisting of thickening and retraction of branches, up to taking a large, ameboid shape, which is accompanied by the elaboration and release of an array of immune mediators, including reactive oxygen and nitrogen species, chemokines, and inflammatory cytokines.[5] Microglia activation is related to the canonical host-defense mechanisms, consisting of the enhancement of phagocytic properties and secretion of trophic factors, which may contribute to neuroprotection and repair. In chronic neuroinflammation, however, microglia remain activated for an extended period, during which the production of inflammatory mediators is sustained longer than usual, thus exacerbating the neural damage.[6] This is particularly evident in neurodegenerative diseases, such as Alzheimer's disease where activated microglia surround extracellular deposits of beta-amyloid and maintain an inflammatory milieu through the secretion of inflammatory cytokines, thus possibly contributing to neuronal death.[7] The contribution of astrocytes to inflammatory processes is much less recognized. However, recent evidence suggests that astrocytes, like

[a]*Fondazione Filarete, viale Ortles 22/4, 20139 Milano, Italy*

[b]*Department of Biotechnology and Translational Medicine, University of Milano, Via Vanvitelli 32, 20129 Milano, Italy. E-mail: michela.matteoli@unimi.it; Fax: +39 02 503 17132*

[c]*Center of Excellence for Neurodegenerative Diseases, University of Milano, Milan, Italy*

[d]*Humanitas Clinical and Research Center, via Manzoni 56, 20089 Rozzano, Italy*

[e]*CIMAINA and Dipartimento di Fisica, Università di Milano, via Celoria 16, I-20133 Milano, Italy*

[f]*CNR-Institute of Neuroscience, via Vanvitelli 32, 20129 Milan, Italy*

† Double first authors.

microglia, can be considered innate-immune-competent cells, with a complex, dual role in the local regulation of immune reactivity. Indeed, astrocytes can react to microbial agents or endogenous danger signals (such as ATP, released from damaged cells) with a unique activation program that controls the local milieu, either promoting inflammation or confining lesions and restoring brain homeostasis.[8] Although it is clear that the ability of glial cells to have positive or negative effects on neuronal survival is context-dependent and that different types of stimulations induce either beneficial or detrimental phenotypes, the factors that initiate this commitment or promote conversion between the two profiles are not completely clarified. In all cases, however, the nature of these stimulating factors was clearly established as a chemical one.

In the last few years it has become clear that not only chemical, but also physical properties of the extracellular environment have a profound influence on cell behavior and differentiation and indeed a combination of micro- and nanoscale chemical and physical extracellular signals appears to regulate cell functions.[9] Cells in their natural environment interact with extracellular matrix components, which are structured at the nanometer scale. As an example, the basement membrane, a ubiquitous component of the extracellular matrix (ECM), possesses a complex mixture of pores, ridges, and fibers with sizes in the nanometer range.[10] Accordingly, cells respond to nanoscale features when grown on synthetic substrates[11–13] and modulation of mechanical stiffness or topography at the nanoscale level has been found to influence cell adhesion and proliferation.[14] The relevance of topographic cues to cell responses is therefore unquestionable. While the nanoscale topographical structure has been found to influence macrophage inflammatory responses,[15] whether and to what extent nanoscale features affect primary glia activation is still undefined. This may have important implications for our understanding of immune activation in the brain, given that physical alteration of the ECM occurs in neurological development and neurodegeneration.[16] Here we show that the nanoscale substrate is sufficient to promote a polarized activation of primary microglia and astrocytes, in a way which is largely independent of the chemical nature of the substrate and differs for the two cell types. We also demonstrate that the nanostructured substrates produce a modulated phenotypic differentiation, which follows the graded nanoscale rugosity.

Results

Substrate characterization

Poly-L-ornithine coated glass has a calculated rms roughness of 0.27 ± 0.020 nm whereas flat titanium dioxide (TiO_2) films (deposited by e-beam evaporation) show an rms roughness of 0.23 ± 0.004 nm. Cluster-assembled nanostructured titanium dioxide (ns-TiO_2) films have a rms roughness of 20.2 ± 0.5 nm and 29.1 ± 1.0 nm respectively (corresponding to 50 nm and 200 nm film thickness). The random stacking of nanoparticles on substrates resulting from supersonic cluster beam deposition (SCBD) produces films with homogeneous nanoscale porosity and roughness: the nanoparticles, landing on the substrate, stick on the surface of the growing film without any relevant diffusion or re-arrangement, as it is typical of a ballistic deposition regime.[17] Ns-TiO_2 substrates were characterized by accurate statistical intraslide/interslide analysis for reproducibility among different production batches and control of their structural and physico-chemical properties.[18] Cell culture media as well as poly-L-ornithine coatings reduce the surface roughness of the nanostructured substrates by about 1.5 nm, however preserving the original surface morphology. Fig. 1 shows Atomic Force Microscopy (AFM) images of buffer coated substrates: (a) ns-TiO_2 film (200 nm thickness), (b) flat TiO_2 film and (c) glass coverslip.

Nanostructured TiO_2 induces changes in microglia shape and enhances microvesicle shedding from the plasma membrane

Primary rat microglia were plated on TiO_2 nanostructured substrates with a roughness of 20 and 29 nm, maintained for 24 hours, and fixed and stained for phalloidin, which labels filamentous actin. Fig. 2a shows that microglia cultured on nanostructured TiO_2 take a round ameboid shape, markedly distinct from the elongated morphology of microglia grown on

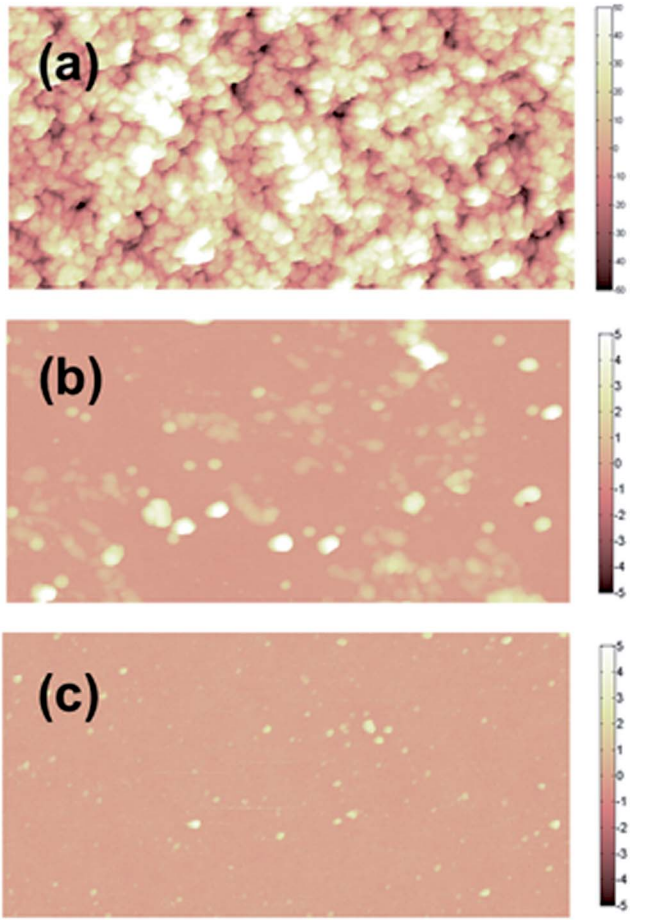

Fig. 1 AFM images of buffer coated substrates: (a) 200 nm thick ns-TiO_2 (2 × 1 μm^2), vertical color scales range between 0 and 120 nm; (b) flat TiO_2 (2 × 1 μm^2), vertical color scales range between 0 and 80 nm and (c) coverslip (2 × 1 μm^2), vertical color scales range between 0 and 40 nm.

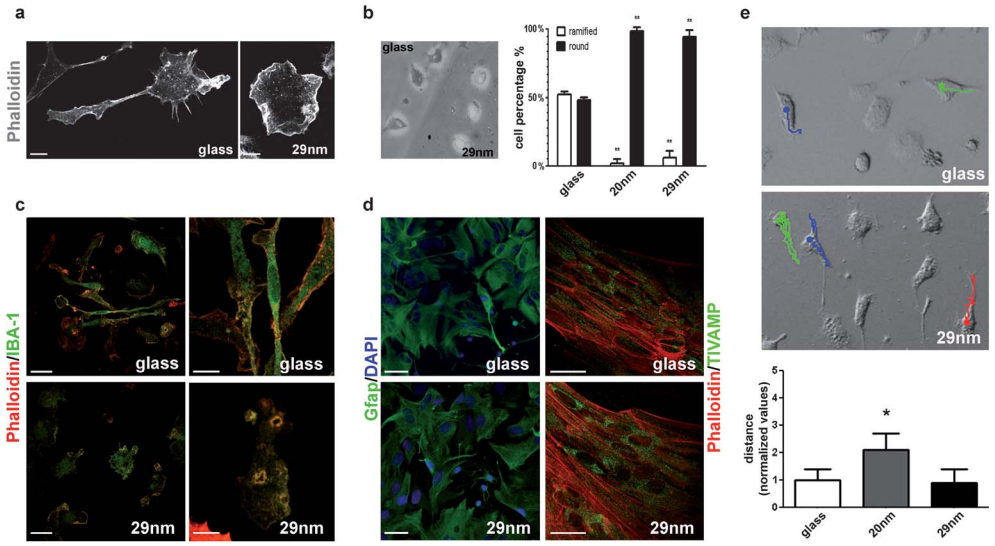

Fig. 2 Morphological and functional changes of primary microglia on TiO_2 nanostructured substrates. (a) Phalloidin staining of the actin cytoskeleton reveals a ramified and elongated morphology of microglia plated on glass (left) and a round ameboid shape of cells plated on 29 nm TiO_2 (right). (b) Bright field image of microglia growing on two sides of a coverslip either covered or not with nanostructured TiO_2. The graph depicts the quantification of the percentage of cells with a round or ramified morphology. (c) Confocal microscopy images of microglial cells stained with phalloidin and anti-IBA1. Note the round morphology of cells plated on nanostructured TiO_2 and the presence of MVs forming from the cell surface. (d) No difference is observed in the morphology of primary astrocytes plated on glass or TiO_2 substrates. (left) GFAP: green and DAPI: blue. (right) Phalloidin: red and TiVAMP: green. (e) Tracking analysis. The paths of cells were determined by the ImageJ Manual Tracking plug-in. Quantification of the mean covered distance reveals that microglia plated on 20 nm TiO_2 display higher mobility (Student's *t*-test, $p < 0.05$). Data are expressed as mean ± SEM and are normalized to control. Calibration bars, (A) and (C) (right): 5 μm, (C) (left) and (D): 25 μm.

polyornithine-coated glass. A similar morphological difference was detected in microglia plated on coverslips only partially coated with nanostructured TiO_2, with microglia plated on TiO_2 showing a more round morphology relative to microglia plated on glass (Fig. 2b). Quantification of the percentage of cells with a round or ramified morphology indicated that the shape switch was induced by TiO_2 substrates with different roughness (Fig. 2b); glass (round = 48% ± 2%; ramified = 52% ± 2%); 20 nm (round = 98% ± 3%; ramified = 2% ± 3%); 29 nm (round = 94% ± 5%; ramified = 6% ± 5%). Staining of cultures for the microglia-specific protein IBA-1 (ionized calcium binding adaptor molecule 1) and phalloidin (Fig. 2c) confirmed the alteration in the morphology and revealed that microglia, grown on nanostructured substrates, display enhanced formation of surface blebs, called microvesicles (MVs), which shed from the cell plasma membrane, representing a new mechanism of cell to cell communication.[19,20] Accordingly, an increased production of MVs was revealed in the extracellular medium by spectrometric analysis (fluorescence arbitrary units, glass: 4430.66 ± 523.40; TiO_2 200 nm: 6195.33 ± 147.87). Differently from microglia, no evident modification in the morphology of primary astrocytes was induced by nanostructured substrates, as revealed by staining for the astrocytic marker Glial Fibrillar Acidic Protein, GFAP, phalloidin, or for the SNARE protein TI-VAMP (tetanus neurotoxin-insensitive vesicle-associated membrane protein) (Fig. 2d). Interestingly, microglia plated on nanostructured substrates displayed a higher mobility, which was specifically detectable at 20 nm roughness (glass = 1 ± 0.41; 20 nm = 2.12 ± 0.60; 29 nm = 0.91 ± 0.49) (Fig. 2e).

Progressive elevation of inflammatory markers in microglia, but not astrocytes, growing on nanostructured substrates with increasing rugosity

Since the change in the morphology from ramified to round as well as production of plasma membrane microvesicles reflect the extent of microglia activation,[21] we assessed whether plating of microglia on nanostructured substrates induced polarization toward a pro-inflammatory phenotype. Analysis of mRNA for the pro-inflammatory enzymes nitric oxide synthase (iNOS) and cyclooxygenase-2 (COX-2) revealed a progressive increase in the expression of the two enzymes in microglia plated on 20 nm TiO_2 and 29 nm TiO_2 as compared to control cells grown on glass, with iNOS increasing more prominently on the 29 nm substrate. Fig. 3 shows representative semiquantitative RT-PCR (Fig. 3a) and quantification of mRNA expression of the two inflammatory markers (Fig. 3b; left, iNOS, qRT-PCR: glass = 1 ± 0.14; 20 nm = 8.21 ± 0.20; 29 nm = 33.95 ± 0.15; right, COX-2, semiquantitative RT-PCR: glass = 1; 20 nm = 1.58 ± 0.25; 29 nm = 2.44 ± 0.44). The increase in iNOS mRNA was paralleled by a large augmentation in nitric oxide (NO) content in microglia grown on a nanostructured substrate, as indicated by the Griess assay, which measures nitrite (NO_2^-), a stable and nonvolatile breakdown product of NO (Fig. 3c; glass = 1 ± 0.0; 20 nm = 2.31 ± 0.18; 29 nm = 8.79 ± 2.36). Notably, an increase in NO production did not occur when microglia were plated on flat TiO_2 (Fig. 3d; glass = 1 ± 0.0; flat = 1.35 ± 0.16), thus indicating that the physical and not the chemical properties of the substrate influence microglia polarization. Acquisition of a pro-inflammatory phenotype by microglia plated on TiO_2 substrates

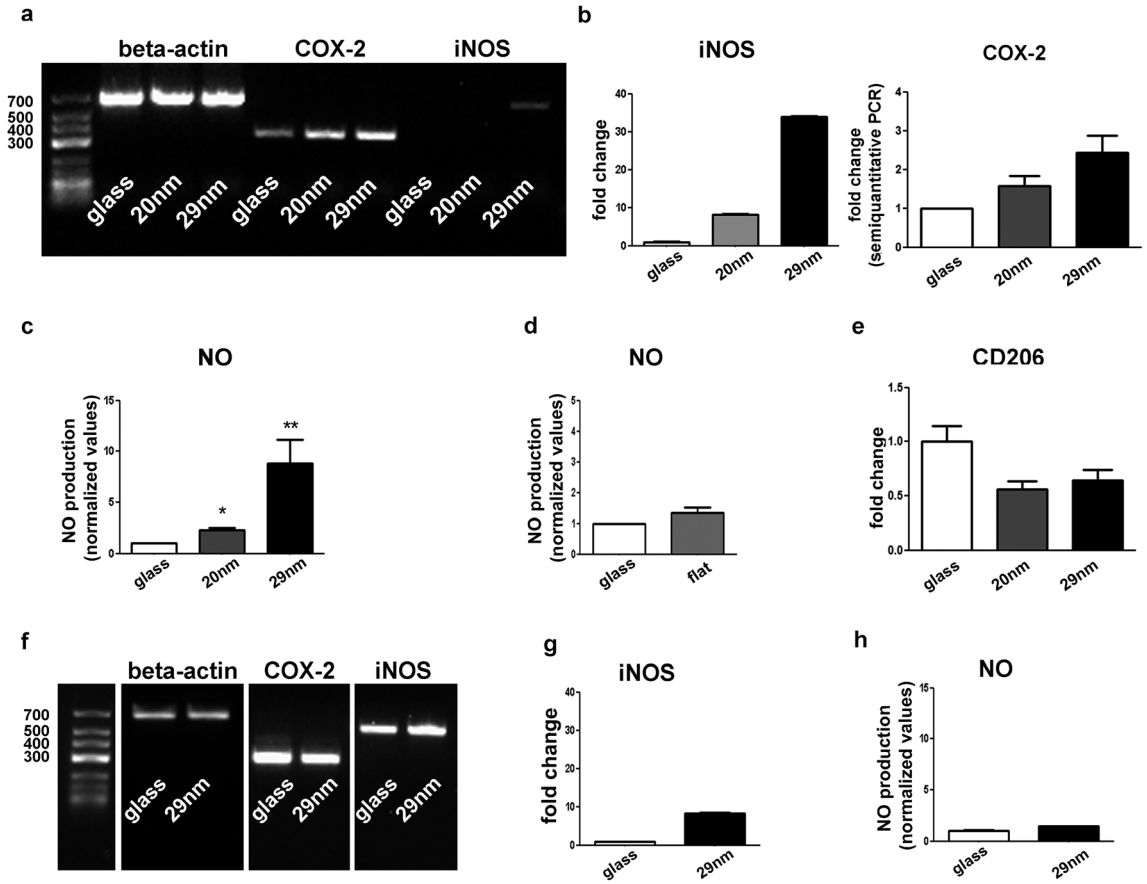

Fig. 3 COX-2 and iNOS expression in microglia and astrocytes growing on nanostructured substrates. (a) Representative semiquantitative PCR of COX-2, iNOS and the housekeeping gene β-actin in microglial cells. (b) Quantification of COX-2 mRNA expression, normalized against the housekeeping gene beta actin (b, right) and qRT-PCR for iNOS transcripts, normalized against the housekeeping gene GAPDH (b, left) in microglia. (c) TiO_2 nanostructured substrates enhance NO production in microglia $^*P < 0.05$; $^{**}P < 0.01$, unpaired Student's *t*-test. (d) Flat TiO_2 coating does not enhance NO production in microglia. (e) Reduced expression of the M2 marker mannose receptor (CD 206) in microglial cells plated on ns-TiO_2 substrates relative to glass as indicated by qRT-PCR. Values represent the mean and range of a representative experiment performed in triplicate. (f) Representative semiquantitative PCR of COX-2, iNOS and the housekeeping gene β-actin in astrocytes. (g) qRT-PCR for iNOS transcripts, normalized against the housekeeping gene GAPDH, in astrocytes. (h) TiO_2 nanostructured substrates do not enhance NO production in astrocytes.

was confirmed by reduced expression of the M2 microglial marker mannose receptor (CD206)[21] (Fig. 3e). Interestingly, a much lower increase of COX-2 and iNOS transcripts (Fig. 3f and g; glass = 1 ± 0.0; 29 nm = 8.27 ± 0.28) and a complete lack of NO content elevation (Fig. 3h; glass = 1 ± 0.10; 200 nm = 1.47 ± 0.02) revealed a lack of relevant changes in primary astrocytes plated on glass *versus* TiO_2 substrates. Significant elevations (several ten-folds) of iNOS expression were instead detected in astrocytes exposed to a cocktail of inflammatory cytokine (IFN-γ, interferon gamma, and TNF-α, tumor necrosis factor-alpha) (not shown), thus confirming that astrocytes are in fact able to up-regulate iNOS upon appropriate stimuli.

In consideration of the prominent increase of COX-2 and iNOS transcripts in microglia, accompanied by the reduction of the anti-inflammatory marker CD 206, ELISA was performed to analyze the relative levels of different cytokines typical of the M1 (inflammatory) or M2 (anti-inflammatory) phenotype in microglia grown under the different experimental conditions. Fig. 4a shows the mean and range from one representative experiment revealing that the expression of four activation markers, *i.e.* the pro-inflammatory cytokine: tumor necrosis factor (TNF)-alpha, the angiogenic factor: Vascular Endothelial Growth Factor (VEGF),[22] the chemotactic chemokine: LIX/CXCL5, produced following stimulation of cells with inflammatory cytokines,[23] and the Fas ligand, a member of the TNF family whose expression is predominantly associated with activated microglia,[24] was increased in microglia grown on nanostructured substrates, with the highest production detectable in microglia grown on 29 nm TiO_2. In all cases, ns-TiO_2 is equally or even more effective than the classical stimulus lipopolysaccharide (LPS) in inducing the conversion of microglia to the proinflammatory, so-called M1, phenotype. Notably, astrocytes grown on the same substrates did not display any increase in these inflammatory markers (Fig. 4b). Furthermore, β-catenin, a central intracellular component of WNT signaling, which increases in microglia undergoing a pro-inflammatory morphogenic transformation in Alzheimer's disease[25] was upregulated, together with its substrate gene c-myc, in microglia grown on nanostructured TiO_2 as assessed by quantitative PCR (Fig. 4c). Notably, no increase in the expression of the same genes was detected in astrocytes plated on the same substrates (Fig. 4d). At variance with proinflammatory markers, where a graded increase in expression occurs between glass,

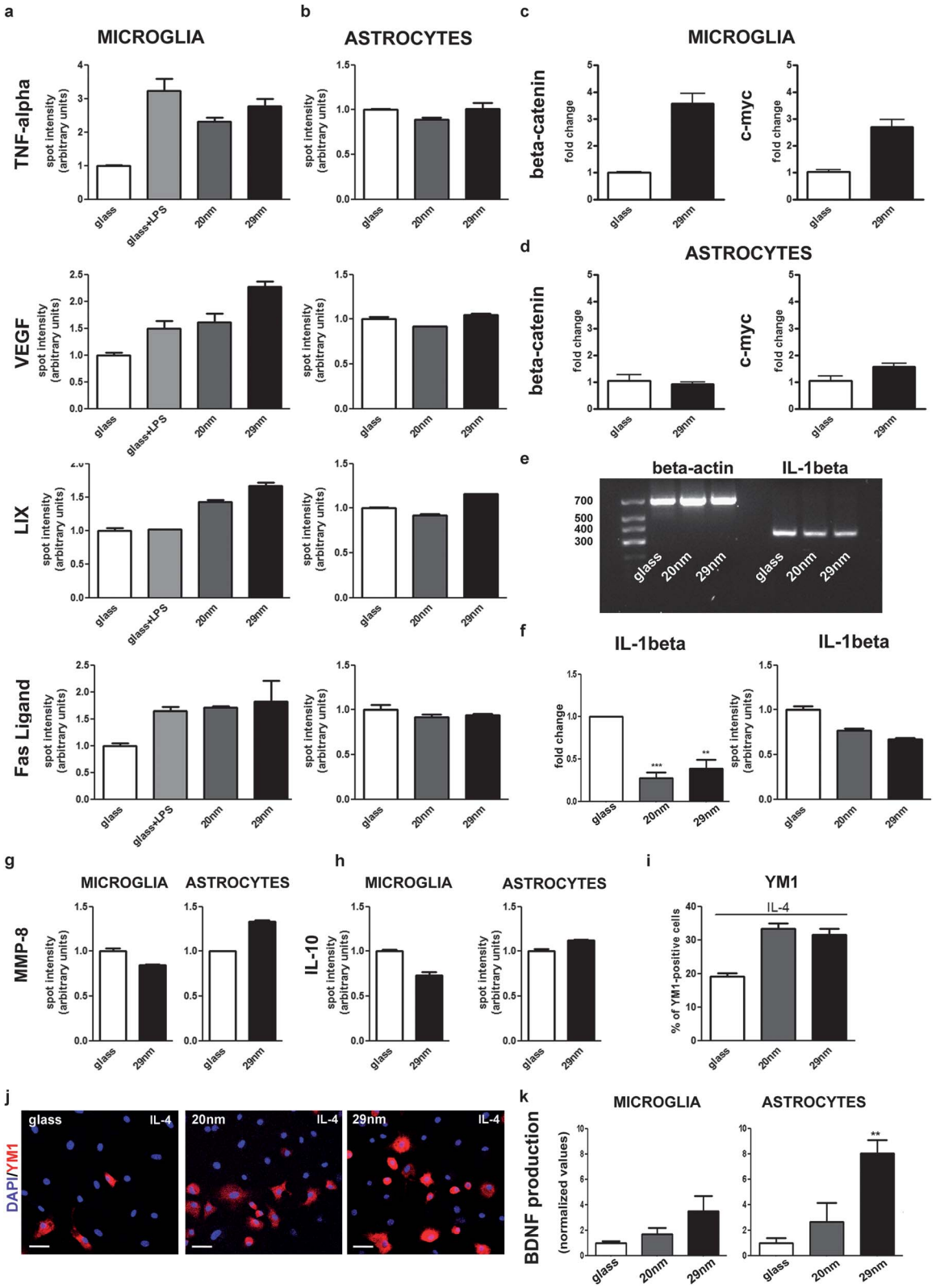

Fig. 4 (a and b) Representative expression pattern of specific pro-inflammatory cytokines. 24 h after seeding, cell lysates were analyzed for expression of a group of 34 cytokines using the RayBio rat cytokine antibody array. Only cytokines with a significant change at the expression level are shown. Values represent the mean and range of a representative experiment performed in duplicate. The results are expressed as arbitrary units. (c and d) RT-PCR analysis showing fold changes in the expression level of β-catenin and c-myc in microglia (c) and astrocytes (d). Semi-quantitative PCR (e), qRT-PCR (f, left) and RayBio analysis (f, right) of IL-1β reveal mild reduction in the cytokine transcript in microglia $^{**}P < 0.01$; $^{***}P < 0.001$, unpaired Student's *t*-test. (g and h) Representative graphs of anti-inflammatory cytokines MMP8 and IL-10 produced by microglia and astrocytes plated on TiO_2 at 29 nm compared to glass, analyzed with the RayBio rat cytokine antibody array. Values represent the mean and range of a representative experiment performed in duplicate. (i) Exposure to IL-4 increases the percentage of YM1-positive mouse microglial cells more prominently in

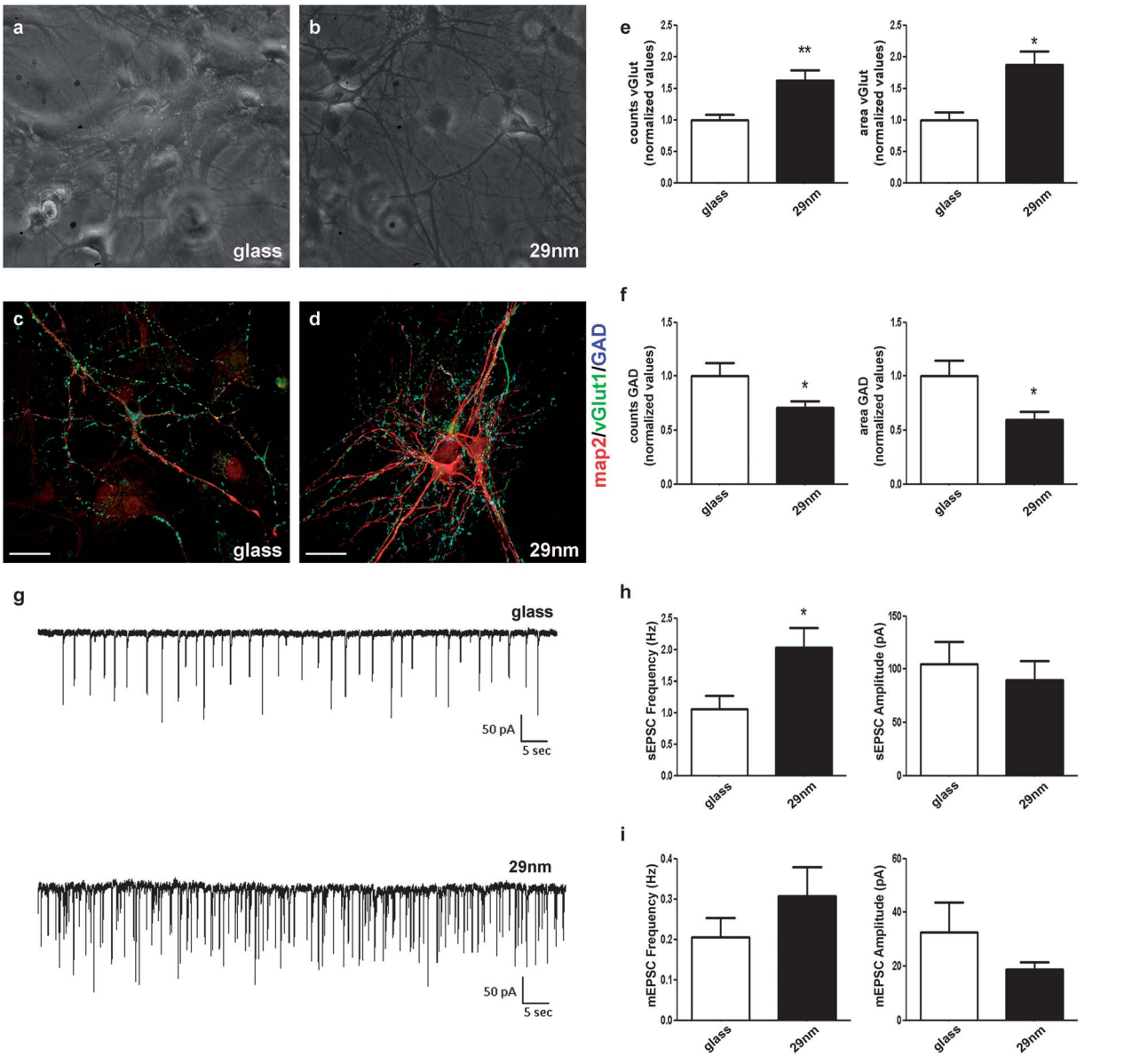

Fig. 5 (a and b) Bright field images of astrocyte–neuron co-cultures plated on glass or a TiO_2 29 nm substrate. (c and d) Representative pictures of neurons co-cultured with astrocytes on glass or a TiO_2 substrate and stained for the dendritic marker MAP2 (red), the vesicular glutamate transporter vGlut1 (green), and the GABA synthesizing enzyme GAD (blue). (e and f) Quantitative analysis of vGlut1 (e) or GAD (f) immunoreactivity in neurons plated on nanostructured TiO_2 or glass. The expression of vGlut1 or GAD has been quantified as the number of positive puncta (left) or total area (right) with the software ImageJ 1.46r. (g) Representative traces of spontaneous EPSCs (sEPSCs) of neurons plated on glass or a TiO_2 substrate. (h) Mean sEPSC frequency and amplitude of control neurons ($n = 17$) and neurons plated on TiO_2 ($n = 17$). $p < 0.05$ *t*-test. (i) Mean miniature EPSC (mEPSC) frequency and amplitude of control neurons ($n = 8$) and neurons plated on TiO_2 ($n = 8$). Calibration bars in (A and B) are 25 μm.

20 nm and 29 nm, a decrease in the expression of the classical pro-inflammatory cytokine interleukin-1β (IL-1β) was demonstrated in microglia growing on TiO_2 substrates by both semi-quantitative (Fig. 4e) or quantitative PCR (glass = 1; 20 nm = 0.27 ± 0.07; 29 nm = 0.39 ± 0.10) (Fig. 4f, left) and multicytokine assay (Fig. 4f, right), with small variations between different substrate rugosities.

Consistent with an inflammatory phenotype induced in primary microglia by nanostructured substrates, the production of anti-inflammatory cytokine interleukin-10 (IL-10) and matrix metalloproteinase-8 (MMP-8), which restrains lung inflammation and inactivates macrophage inflammatory protein-1 alpha,[26] was reduced in microglia growing on TiO_2 with 29 nm rugosity (Fig. 4g and h). Notably, however, when microglia were

cultures grown on ns-TiO_2 relative to glass. (j) YM1 and DAPI staining of mouse microglial cells reveals a higher number of positive cells on ns-TiO_2 compared to glass. Calibration bar: 25 μm. (k) The level of BDNF production was measured from cell lysates using an ELISA assay kit. Note the increase in BDNF production in astrocytes plated on TiO_2 $^{**}P > 0.01$, unpaired Student's *t*-test.

exposed to a chemical stimulus which favors the polarization toward the M2 alternatively activated phenotype, the phenotypic conversion was enhanced by the simultaneous exposure to ns-TiO_2. Indeed, a significantly higher percentage of microglial cells positive for the M2 marker YM1 was detected, upon exposure to IL-4, in microglia grown on ns-TiO_2 relative to glass (Fig. 4i and j). These data suggest that, while microglia exposure to ns-TiO_2 favours, by default, the differentiation toward an inflammatory phenotype, the physical stimulus may synergize with positive chemical signals to produce alternatively activated, anti-inflammatory profiles. Conversely, no reduction, but instead a slight increase in the expression of the anti-inflammatory markers was observed in primary astrocytes grown on nanostructured substrates (Fig. 4g and h). Furthermore, astrocytes grown on nanostructured substrates potently upregulated, at the protein level, the expression of the growth factor brain-derived neutrophic factor (BDNF) which has pleiotropic effects on neuronal development, including promotion of axonal regeneration and reconstruction after injury in the adult CNS.[27,28] In particular, primary astrocytes grown on 29 nm TiO_2 increased by around 8-fold the expression of BDNF as assessed by ELISA (Fig. 4k; glass = 1 ± 0.37; 20 nm = 2.64 ± 1.50; 29 nm = 8.04 ± 1.05). A more modest increase in BDNF expression was observed in microglia (Fig. 4k; glass = 1 ± 0.13; 20 nm = 1.66 ± 0.52; 29 nm = 3.51 ± 1.16).

As a further support to the production of regenerative factors by astrocytes grown on nanostructured substrates, neurons plated on top of astrocytes growing on nanostructured TiO_2 displayed increased synaptogenesis. Staining of cultures for the excitatory marker vGlut1 (vesicular glutamate transporter 1) and for the inhibitory marker GAD (glutamic acid decarboxylase) (Fig. 5a–d) revealed that nanostructured TiO_2-plated astrocytes enhance glutamatergic synaptogenesis (Fig. 5e; counts vGlut1: glass = 1 ± 0.09; 29 nm = 1.62 ± 0.16; area vGlut1: glass = 1 ± 0.12; 29 nm = 1.87 ± 0.20). Also, a significant difference in the extent of inhibitory synaptogenesis was observed (Fig. 5f; counts GAD: glass = 1 ± 0.12; 29 nm = 0.71 ± 0.06; area GAD: glass = 1 ± 0.14; 29 nm = 0.60 ± 0.07). These data were confirmed by electrophysiological recordings of synaptic activity in neurons plated on top of astrocytes grown on nanostructured TiO_2 or glass (Fig. 5g), which revealed a higher frequency of spontaneous excitatory postsynaptic currents sEPSCs (Fig. 5h; sEPSC frequency, glass = 1.06 ± 0.22; 29 nm = 2.03 ± 0.32; sEPSC amplitude, glass = 104.89 ± 21.16; 29 nm = 89.72 ± 18.34) and of miniature excitatory postsynaptic currents mEPSCs (Fig. 5i; mEPSC frequency, glass = 0.21 ± 0.05; 29 nm = 0.31 ± 0.07; mEPSC amplitude, glass = 32.51 ± 11.24; 29 nm = 18.65 ± 2.71). No significant changes in either sEPSC or mEPSC amplitudes were observed. These data confirm that neurons plated on top of astrocytes grown on TiO_2 form a higher number of synapses relative to glass co-cultures.

Discussion

Different cellular properties, including cell migration and proliferation, can be altered by the physical properties of the substrate, such as its surface roughness and wettability. In particular, nanostructured materials induce the activation of focal adhesion kinases, integrin-mediated focal adhesion and actin stress fibers in endothelial cells[29,30] while in PC12 cells, the roughness of nanostructured TiO_2 triggers neuritogenesis by activating the expression of nitric oxide synthase (NOS) and the consequent nitration of cytoskeletal proteins.[31] Furthermore, nanoscale surface features appear to regulate macrophage production of nitric oxide synthase (iNOS), in a manner similar to lipopolysaccharide (LPS) and other inflammatory cytokines.[15,32]

Despite the increasing amount of data indicating that the nanoscale substrate topography influences cell adhesion, proliferation and differentiation,[33] no evidence has been provided of whether primary cells from brain modify their functional profile in relation to the nanoscale features of environmental cues. This is a major issue to be addressed, as the extracellular matrix with which brain cells interact includes topography at the nanoscale, and such topography may be altered under pathological conditions. As an example, aberrant components of the extracellular matrix are associated with the pathological hallmarks of Alzheimer's disease, *i.e.* plaques and tangles and, in particular, the pattern and abundance of membrane-bound heparan sulfate proteoglycans (HSPGs) suggest an early association with neurodegeneration.[16]

Our study shows that nanostructured substrates are able, exclusively in virtue of their physical properties, to push primary brain microglia toward the pro-inflammatory activation phenotype, with an efficacy which reflects the nanoscale roughness. The induction of the pro-inflammatory profile is more prominent in microglia grown on 29 nm roughness relative to 20 nm rough nanostructured substrates. These data are in line with a recent study performed on the murine-macrophage cell-line RAW264 plated on nanoscale grooved substrates showing that the nanoscale grooves, and in particular the 150 nm pitch, may specifically induce a mild inflammatory response, able to promote wound-healing response.[15] Among the proteins and enzymes whose expression was more potently induced in microglia plated on nanostructured substrates with higher roughness, we detected iNOS, TNF-alpha, VEGF, LIX/CXCL5 and Fas ligand, *i.e.* markers whose expression is predominantly associated with activated microglia.[34–36] Unexpectedly, although nanostructured substrates induce the expression of inflammatory cytokines in microglia, we could not detect any increase, but actually a slight decrease, in production of the pro-inflammatory cytokine IL-1β. IL-1β has been proved to play a role in inducing iNOS expression.[37] Also it has been shown to be responsible for increasing microglial motility.[38] Our data, indicating the lack of IL-1β increase in microglia grown on nanostructured substrates, exclude the involvement of IL-1β in the TiO_2-induced enhancement of iNOS activity as well as in the increased motility of microglia on nanostructured substrates.

The pathway by which the nanoscale substrate induces an inflammatory phenotype in microglial cells is still undefined. Notably, we excluded the involvement of integrins, since the integrin-blocking RGD peptides[39,40] were unable to inhibit the induction of the pro-inflammatory phenotype in microglia plated on nanostructured substrates (our unpublished observations). Interestingly, however, we found an enhancement in the

expression of beta catenin and its substrate c-myc in microglia grown on nanostructured substrates. This suggests a possible involvement of signalling by the Wnt family of secreted glycolipoproteins, a known mechanism that controls key developmental gene expression programs.[41] Previous studies have shown that peripheral macrophages can employ Wnt-based communication to modulate inflammatory responses,[42] thus suggesting that brain microglia could also process Wnt signals. In line with this possibility, the occurrence of increased β-catenin levels in microglia transiting from a surveying to an active macrophage-like stage in post-mortem AD brains has been previously demonstrated.[25] These data suggest that enhanced β-catenin signaling may occur in the inflammatory transformation of microglia and possibly participate in the exacerbation of AD-related neuroinflammation. Notably, a Wnt-induced microglia response is characterized by the increased expression of inducible nitric oxide synthase, cyclooxygenase-2, cytokines, chemokines and enhanced invasive capacity,[43] all features that we replicate using nanostructured substrates. The cellular processes by which microglia plated on nanostructured substrates may display an enhanced Wnt/beta catenin signaling are still to be defined. Interestingly, however, it has been shown recently that Wnts, in order to signal target cells, travel in the extracellular space through extracellular vesicles of exosomal origin.[44] Our demonstration that formation of extracellular vesicles is increased when microglia are plated on nanostructured substrates may suggest the occurrence of a potentiated release[45] and long-range signaling of Wnt molecules. Interestingly, no increase in beta-catenin expression was detected in primary astrocytes growing on nanostructured substrates. The fact that different cell types respond very differently to surface topography has been shown by several groups. As an example, increasing surface roughness decreased fibroblast proliferation rate and increased osteoblast proliferation.[46] Also, osteoblast differentiation was increased on a surface with low roughness, whereas chondrocytic differentiation was increased on a rough surface.[9,47] Therefore, the importance of topographic cues varies for different cell types. Accordingly we demonstrate that astrocytes do not enhance the expression of pro-inflammatory markers when plated on nanostructured materials, but increase, to different extents, the production of anti-inflammatory and regenerative factors. In particular, 29 nm rough substrates slightly increase the production of the anti-inflammatory factors IL-10 and MMP-8, as well as the production of ciliary neurotrophic factor (CNTF), a potent survival factor for neurons (not shown) and, more prominently, that of BDNF, a member of the "neurotrophin" family of growth factors which supports the survival of existing neurons and favors the growth and differentiation of new neurons and synapses.[48] Consistently, enhanced synaptogenesis and synaptic activity is clearly detectable in neurons growing on top of astrocytes plated on nanostructured substrates.

Experimental procedures

Substrates

Poly-ornithine coated glass coverslips (Colaver, 64MU4113) were used as reference samples for cell culture. Cluster-assembled ns-TiO_2 substrates were grown on glass slides by Supersonic Cluster Beam Deposition (SCBD) using a Pulsed Microplasma Cluster Source (PMCS), as described in detail.[49] Briefly, the PMCS operation principle is based on the ablation of a titanium rod by argon plasma, ignited by a pulsed electric discharge.[50] The ablated species thermalize with the argon and condense to form clusters. The mixture of clusters and inert gas is then extracted in a vacuum through an aerodynamical focusing assembly to form a seeded supersonic beam,[51] the clusters are then collected on a substrate located in the beam trajectory. Since the clusters' kinetic energy is low enough to avoid fragmentation, the nanoparticles impinging on the substrates maintain their original structure and, *via* random stacking, a nanostructured film is grown.[52] The deposition process takes place under high vacuum thus allowing the partial oxidation of the Ti clusters, further oxidation is obtained upon air exposure to atmospheric conditions and it is completed with mild annealing for two hours at the temperature of 250 °C under a continuous flux of dry air. The annealing procedure has the further purpose of removing adsorbed species from the sample surfaces.

Flat TiO_2 films were grown on glass slides by electron beam evaporation of a titanium target. The evaporated metal was partially oxidized during the deposition and almost fully oxidized upon subsequent air exposure. Film thickness was measured by Contact Stylus Profilometry (Dektak Veeco); the surface morphology was characterized by atomic force microscopy (AFM-Digital Instruments Nanoscope multimode IV). The AFM is equipped with rigid cantilevers with single-crystal silicon tips (nominal radius 5–10 nm) and operated in Tapping Mode. Typically, several (4–6) 2 μm × 1 μm images (2048 × 1024 points) were acquired on each sample, and flattened by line-by-line subtraction of first and second-order polynomials in order to eliminate the tilt of the sample and of the scanner bow. From the flattened AFM images, the average nanoscale root-mean-square roughness and specific area parameters were calculated.

Cell culture

Astrocytes were prepared from post-natal day 2 (P2) Sprague Dawley rat or C57Bl/6 mouse cerebral tissue (Charles River, Wilmington, MA) as described by Verderio and colleagues (2012).[21] Cells were maintained in MEM medium containing 10% FBS. After 3 weeks, in order to collect microglial cells, the cultures were shaken on a rotary shaker (200 rpm) at RT for 30 min. Microglial cells were maintained as described.[21] In a set of experiments, microglial cells were stimulated with 0.4 μg ml^{-1} lipopolysaccharide (LPS, Sigma-Aldrich, St. Louis, MO) for 6 h to drive the M1 proinflammatory phenotype, or with 10 ng ml^{-1} IL-4 (Sigma-Aldrich, St. Louis, MO) for 48 h to polarize cells toward the M2 alternatively activated phenotype.

Rat or mouse hippocampal neurons were established from fetal E18 Sprague Dawley rats or C57bl/6 mice (Charles River, Wilmington, MA), respectively. The dissociated cells were plated onto titanium-treated coverslips and maintained in Neurobasal (Gibco, Life Technologies Ltd., Paisley, UK) with 2% B27 supplement (Gibco, Life Technologies Ltd., Paisley, UK).

Neuronal cultures seeded on poly-L-lysine-treated coverslips and maintained under the same conditions were used as a control. All efforts were made to minimize animal suffering and to reduce the number of animals used, in accordance with the European Communities Council Directive of September 20, 2010 (2010/63/UE). All procedures involving animals were performed according to the guidelines of the Institutional Animal Care and Use Committee of the University of Milan.

Quantification of MV shedding

Microglia plated on different nanosubstrates were labeled with the fluorescent styryl dye FM1–43 (2 μM) for 2 min, extensively washed and exposed for 20 min to 1 mM ATP in Kreb's Ringer solution. The extracellular saline was collected and centrifuged at 300 g for 5 minutes to remove detached cells. To quantify the amount of FM1–43-labeled MVs, shed in to the extracellular saline, the total green fluorescence of the resulting supernatant was then assayed at 485/535 nm and 10 Hz with a spectrophotometric system (1420 Multilabel Counter Victor 2; Wallac) as described previously.[19] Data measurements were presented as fluorescent arbitrary units.

Semiquantitative PCR

Aliquots (5–15% of the reverse-transcribed cDNA product) of total cDNA were amplified in each PCR assay with FastStart Taq DNA Polymerase (Roche Diagnostics, Indianapolis, IN, USA) in a total volume of 25 μl of reaction mixture containing 0.5 μM of 5′ and 3′ primers in a standard PCR buffer (50 mM Tris–HCl, 10 mM KCl, 5 mM $(NH_4)_2SO_4$, 2 mM $MgCl_2$, pH 8.3). Control samples lacking cDNA were processed in parallel with the same experimental protocol. All PCR reagents were purchased from Applied Biosystems (Life Technologies Ltd., Paisley, UK). Amplifications were performed using a 2720 thermal cycler (Applied Biosystems, Life Technologies Ltd., Paisley, UK). The oligonucleotide primers used for β-actin (internal control) were 5′-CTAGAAGCATTGCGGTGGACGATGGAGGG-3′ (sense) and 5′-TGACGGGGTCACCCACACTGTGCCCATCTA-3′ (antisense); these primers generate a 659bp PCR fragment. Primers used for iNOS were 5′-AAGTCCAGCCGCACCACCCT-3′ (sense) and 5′-TGCAGACGCCATGGTGCAGG-3′ (antisense) 595bp; COX-2 5′-GAGCACCTGCGGTTCGCTGT-3′ (sense) and 5′-GCAGCAGCGGATGCCAGTGA-3′ (antisense) 334bp; IL-1β 5′-CAGGAAGGCAGTGTCACTC-3′ (sense) and 5′-GGGATTTTGTCGTTGCTTGT-3′ (antisense) 339bp.

Real-time quantitative RT-PCR

Total cellular RNA was extracted 24 h (microglia) or 7 days (astrocytes) after seeding using Trizol reagent (Invitrogen, Life Technologies Ltd., Paisley, UK) according to the manufacturer's specifications. Superscript III reverse transcriptase (Invitrogen, Life Technologies Ltd., Paisley, UK) was used to generate cDNA using 1 μg of RNA and random examers or oligo dT primer, according to the manufacturer's instructions. The relative expression of iNOS, IL-1β, beta-catenin and c-myc gene was assessed, using the 7900 HT fast-real-time PCR system instrument (Applied Biosystems, Life Technologies Ltd., Paisley, UK). The PCR reactions were run with 5 μl of cDNA in a total volume of 11 μl, using TaqMan Gene Expression Master Mix (Applied Biosystems, Life Technologies Ltd., Paisley, UK) and predesignated TaqMan Gene Expression Assay from PE Applied Biosystems. Amplification reactions were carried out in triplicate for each examined sample. Expression data were normalized to the housekeeping gene GAPDH to control the variability in expression levels and were analyzed using the ΔΔCt method.

Cytokine antibody array

A rat cytokine antibody array (Raybiotech Inc., Norcross, GA, USA) was used to simultaneously detect and quantify 34 cytokines in samples collected from astrocytes and microglia cells. After lysis with 2× RayBio® Cell Lysis Buffer, the protein concentrations were analyzed by BCA. The cytokine antibody array was performed according to the manufacturer's instructions. The signals were detected using the ECL kit according to the user manual. The membranes were exposed to an X-ray film (Amersham Hyperfilm ECL, GE Healthcare, UK) and the film was scanned for densitometry analysis using the BioRad GS-800 Calibrated Densitometer (Bio-Rad, Hercules, CA). The resulting images were analyzed with ImageJ software to determine the integrated density value of each protein spot. Densitometry data were normalized to internal positive controls on each membrane and graphed as relative units.

Griess assay

Quantification of NO production was performed using a Griess reagent kit (G7921, Invitrogen, Life Technologies Ltd., Paisley, UK) following manufacturer's instructions. Briefly, 150 μl of cell lysates were allowed to react with 150 μl of Griess reagent and were incubated at room temperature for 30 min. Samples absorbance was measured using a Tecan Infinite F500 plate reader (Tecan Group Ltd., Männedorf, Switzerland) at 548 nm. Lysis solution served as the blank in all experiments.

Enzyme immunoassay of BDNF (ELISA)

A BDNF Immunoassay system (Promega, Italy) was used to quantify the production of neurotrophin from microglia and astrocytes. BDNF in cell lysates was measured following the manufacturer's instructions. Sample absorbance was measured with a Tecan Infinite F500 plate reader at 450 nm (Tecan Group Ltd., Männedorf, Switzerland).

Immunocytochemistry

Cell cultures were fixed for 20 min at room temperature with 4% paraformaldehyde in 0.12 M phosphate buffer containing 0.12 M sucrose. The following antibodies were used: mouse anti-GFAP (Sigma Aldrich, St. Louis, MO), 1 : 500; rabbit anti-IBA-1 (Wako Chemicals GmbH, Neuss, Germany), 1 : 100; mouse anti-TI-VAMP (produced by T. Galli, INSERM, Paris), 1 : 100; DAPI (Molecular Probes, Life Technologies Ltd., Paisley, UK); mouse anti-MAP2 (Synaptic System GmbH, Goettingen, Germany), 1 : 300; guinea pig anti-vGlut1 (Synaptic System GmbH, Goettingen, Germany), 1 : 1000; human anti-GAD

serum (kind gift of M. Solimena, Dresden University), 1 : 200; rabbit anti-T-lymphocyte-derived eosinophil chemotactic factor (YM1; Stemcell Technologies Inc., Vancouver, Canada), 1 : 100. Actin filaments were stained with Alexa Fluor 568-conjugated phalloidin (Invitrogen, Life Technologies Ltd., Paisley, UK), 1 : 300. Secondary antibodies were conjugated with Alexa-488, Alexa-555 or Alexa-633 fluorophores (Invitrogen, Life Technologies Ltd., Paisley, UK). Images were acquired using a Leica SPE confocal microscope equipped with an ACS APO 63×/1.30 or an ACS APO 40×/1.15 oil objective.

Manual tracking

An ImageJ plug-in "MTrackJ" was used to manually track migration paths of microglia. To this end, the cell soma was identified at each time point in the optical section. For each cell and time point the software calculated migration length (μm) and velocity (μm min^{-1}). Only cells present in the field of view for 1 hour were included in the analysis. Data were exported to MS Excel and the mean per cell was calculated. In addition, absolute values of migration length between successive time points were computed for *X* and *Y* coordinates.

Electrophysiology

Whole cell voltage-clamp recordings of spontaneous synaptic activity were performed on rat embryonic hippocampal neurons maintained in culture for 9–12 DIV. Patch pipettes (2–4 MΩ) were pulled using a micropipette electrode puller (Sutter Instruments) and filled with internal recording solution containing (in mM): KGluc 130; EGTA 1; KCl 10; $MgCl_2$ 2; HEPES 10; mg ATP 40; Tris-GTP 3 (pH 7.3). Cells plated on glass or TiO_2 substrates were placed in a recording chamber perfused continuously with extracellular solution containing (in mM): NaCl 125; KCl 5; $MgSO_4$ 1.2; $CaCl_2$ 2; $KHPO_4$ 1.2; HEPES 25; Glu 6 (pH 7.3). Recordings were conducted at −70 mV. For mEPSC recordings TTX (1 μM) was added to the extracellular solution. Series resistance ranged from 10 to 20 MΩ and was monitored for consistency during recordings. Recordings with leak currents >100 pA were excluded from our analysis. Signals were recorded using Multiclamp 700B amplifiers and digitized with Digidata 1440 (Axon Instruments, Molecular devices). Signals were amplified, sampled at 10 kHz, filtered to 2 or 3 kHz, and analyzed using the pClamp 10 data acquisition and analysis program.

Statistical analysis

All data are presented as mean or median ± standard deviation or SE from the indicated number of experiments. Data were compared using the Student's *t*-test for parametric data or one-way ANOVA. The differences were considered to be significant if $P < 0.05$ and are indicated by an asterisk, those at $P < 0.01$ are indicated by double asterisks and those at $P < 0.001$ are indicated by triple asterisks.

Conclusions

In conclusion, our study defines the role of nanoscale morphology as a biomaterial design parameter to dissect the molecular mechanisms involved in the activation of inflammatory pathways in brain cells. Besides representing potentially relevant findings for those applications where nanostructures interact with biological systems, these results importantly contribute to our understanding of brain function in health and disease. Indeed, by demonstrating that not only chemical inputs, but also physical stimuli may be sufficient to induce immune activation of microglia in the brain, they open the possibility that extracellular matrix nanoscale components, which are known to undergo changes during neuropathological states, may contribute to modulation of microglia states. In this respect they open novel avenues for dissecting the mechanisms involved in brain diseases and for potentially identifying novel therapeutic targets.

Acknowledgements

We wish to thank Dr Elena Turola and Dr Fabia Filipello (University of Milan) for help in some experiments, and Dr Elisabetta Menna (CNR, IN) and Prof. Gabriella Tedeschi (University of Milano) for discussion. We wish to thank Fondazione Filarete for supporting the research which has led to the present results. The research has also been partially supported by EU-FP7 European project SaveMe (CP-IP 263307-2) to MM and PM, Cariplo 2011-2117 to MM, PM and CL, and Cariplo 2011-2114 to CV.

References

1 T. Schlegelmilch, K. Henke and F. Peri, Microglia in the developing brain: from immunity to behaviour, *Curr. Opin. Neurobiol.*, 2011, **21**(1), 5–10.
2 D. Davalos, J. Grutzendler, G. Yang, J. V. Kim, Y. Zuo, S. Jung, D. R. Littman, M. L. Dustin and W. B. Gan, ATP mediates rapid microglial response to local brain injury *in vivo*, *Nat. Neurosci.*, 2005, **8**(6), 752–758.
3 A. Nimmerjahn, F. Kirchhoff and F. Helmchen, Resting microglial cells are highly dynamic surveillants of brain parenchyma *in vivo*, *Science*, 2005, **308**(5726), 1314–1318.
4 H. Wake, A. J. Moorhouse, S. Jinno, S. Kohsaka and J. Nabekura, Resting microglia directly monitor the functional state of synapses *in vivo* and determine the fate of ischemic terminals, *J. Neurosci.*, 2009, **29**(13), 3974–3980.
5 R. B. Banati, The immune response in the Alzheimer's disease brain, *Biochem. Soc. Trans.*, 1997, **25**(2), 683–685.
6 R. M. Ransohoff and A. E. Cardona, The myeloid cells of the central nervous system parenchyma, *Nature*, 2010, **468**(7321), 253–262.
7 V. H. Perry, J. A. Nicoll and C. Holmes, Microglia in neurodegenerative disease, *Nat. Rev. Neurol.*, 2010, **6**(4), 193–201.

8 C. Farina, F. Aloisi and E. Meinl, Astrocytes are active players in cerebral innate immunity, *Trends Immunol.*, 2007, **28**(3), 138–145.
9 E. K. Yim and K. W. Leong, Significance of synthetic nanostructures in dictating cellular response, *Nanomedicine*, 2005, **1**(1), 10–21.
10 G. A. Abrams, S. L. Goodman, P. F. Nealey, M. Franco and C. J. Murphy, Nanoscale topography of the basement membrane underlying the corneal epithelium of the rhesus macaque, *Cell Tissue Res.*, 2000, **299**(1), 39–46.
11 M. J. Dalby, M. O. Riehle, H. Johnstone, S. Affrossman and A. S. Curtis, *In vitro* reaction of endothelial cells to polymer demixed nanotopography, *Biomaterials*, 2002, **23**(14), 2945–2954.
12 A. S. Andersson, F. Backhed, A. von Euler, A. Richter-Dahlfors, D. Sutherland and B. Kasemo, Nanoscale features influence epithelial cell morphology and cytokine production, *Biomaterials*, 2003, **24**(20), 3427–3436.
13 A. Thapa, T. J. Webster and K. M. Haberstroh, Polymers with nano-dimensional surface features enhance bladder smooth muscle cell adhesion, *J. Biomed. Mater. Res., Part A*, 2003, **67**(4), 1374–1383.
14 E. K. Yim, E. M. Darling, K. Kulangara, F. Guilak and K. W. Leong, Nanotopography-induced changes in focal adhesions, cytoskeletal organization, and mechanical properties of human mesenchymal stem cells, *Biomaterials*, 2010, **31**(6), 1299–1306.
15 E. Lamers, X. F. Walboomers, M. Domanski, L. Prodanov, J. Melis, R. Luttge, L. Winnubst, J. M. Anderson, H. J. Gardeniers and J. A. Jansen, *In vitro* and *in vivo* evaluation of the inflammatory response to nanoscale grooved substrates, *Nanomedicine*, 2012, **8**(3), 308–317.
16 D. Bonneh-Barkay and C. A. Wiley, Brain extracellular matrix in neurodegeneration, *Brain Pathol.*, 2009, **19**(4), 573–585.
17 A. Podestà, G. Bongiorno, P. E. Scopelliti, S. Bovio and P. Milani, Cluster-assembled nanostructured titanium oxide films with tailored wettability, *J. Phys. Chem. C*, 2009, **113**, 18264–18269.
18 R. Carbone, M. De Marni, A. Zanardi, S. Vinati, E. Barborini, L. Fornasari and P. Milani, Characterization of cluster-assembled nanostructured titanium oxide coatings as substrates for protein arrays, *Anal. Biochem.*, 2009, **394**(1), 7–12.
19 F. Bianco, E. Pravettoni, A. Colombo, U. Schenk, T. Moller, M. Matteoli and C. Verderio, Astrocyte-derived ATP induces vesicle shedding and IL-1 beta release from microglia, *J. Immunol.*, 2005, **174**(11), 7268–7277.
20 E. Turola, R. Furlan, F. Bianco, M. Matteoli and C. Verderio, Microglial microvesicle secretion and intercellular signaling, *Front. Physiol.*, 2012, **3**, 149.
21 C. Verderio, L. Muzio, E. Turola, A. Bergami, L. Novellino, F. Ruffini, L. Riganti, I. Corradini, M. Francolini, L. Garzetti, C. Maiorino, F. Servida, A. Vercelli, M. Rocca, D. Dalla Libera, V. Martinelli, G. Comi, G. Martino, M. Matteoli and R. Furlan, Myeloid microvesicles are a marker and therapeutic target for neuroinflammation, *Ann. Neurol.*, 2012, **72**(4), 610–624.
22 S. D. Croll, R. M. Ransohoff, N. Cai, Q. Zhang, F. J. Martin, T. Wei, L. J. Kasselman, J. Kintner, A. J. Murphy, G. D. Yancopoulos and S. J. Wiegand, VEGF-mediated inflammation precedes angiogenesis in adult brain, *Exp. Neurol.*, 2004, **187**(2), 388–402.
23 S. Struyf, P. Proost and J. Van Damme, Regulation of the immune response by the interaction of chemokines and proteases, *Adv. Immunol.*, 2003, **81**, 1–44.
24 Y. M. Lu, R. R. Tao, J. Y. Huang, L. T. Li, M. H. Liao, X. M. Li, K. Fukunaga, Z. H. Hong and F. Han, P2X(7) signaling promotes microsphere embolism-triggered microglia activation by maintaining elevation of Fas ligand, *J. Neuroinflammation*, 2012, **9**, 172.
25 C. Halleskog, J. Mulder, J. Dahlstrom, K. Mackie, T. Hortobagyi, H. Tanila, L. Kumar Puli, K. Farber, T. Harkany and G. Schulte, WNT signaling in activated microglia is proinflammatory, *Glia*, 2011, **59**(1), 119–131.
26 P. A. Quintero, M. D. Knolle, L. F. Cala, Y. Zhuang and C. A. Owen, Matrix metalloproteinase-8 inactivates macrophage inflammatory protein-1 alpha to reduce acute lung inflammation and injury in mice, *J. Immunol.*, 2010, **184**(3), 1575–1588.
27 J. Y. Zhang, X. G. Luo, C. J. Xian, Z. H. Liu and X. F. Zhou, Endogenous BDNF is required for myelination and regeneration of injured sciatic nerve in rodents, *Eur. J. Neurosci.*, 2000, **12**(12), 4171–4180.
28 J. C. Wilhelm, M. Xu, D. Cucoranu, S. Chmielewski, T. Holmes, K. S. Lau, G. J. Bassell and A. W. English, Cooperative roles of BDNF expression in neurons and Schwann cells are modulated by exercise to facilitate nerve regeneration, *J. Neurosci.*, 2012, **32**(14), 5002–5009.
29 J. Y. Lim, A. D. Dreiss, Z. Zhou, J. C. Hansen, C. A. Siedlecki, R. W. Hengstebeck, J. Cheng, N. Winograd and H. J. Donahue, The regulation of integrin-mediated osteoblast focal adhesion and focal adhesion kinase expression by nanoscale topography, *Biomaterials*, 2007, **28**(10), 1787–1797.
30 H. S. Hung, C. C. Wu, S. Chien and S. H. Hsu, The behavior of endothelial cells on polyurethane nanocomposites and the associated signaling pathways, *Biomaterials*, 2009, **30**(8), 1502–1511.
31 M. Tamplenizza, C. Lenardi, E. Maffiola, S. Nonnis, A. Negri, S. Forti, E. Sogne, S. De Astis, M. Matteoli, P. Milani and G. Tedeschi, *J. Nanobiotechnol.*, 2013, in press.
32 A. K. Refai, M. Textor, D. M. Brunette and J. D. Waterfield, Effect of titanium surface topography on macrophage activation and secretion of proinflammatory cytokines and chemokines, *J. Biomed. Mater. Res., Part A*, 2004, **70**(2), 194–205.
33 I. Wheeldon, A. Farhadi, A. G. Bick, E. Jabbari and A. Khademhosseini, Nanoscale tissue engineering: spatial control over cell-materials interactions, *Nanotechnology*, 2011, **22**(21), 212001.
34 J. K. Krady, A. Basu, C. M. Allen, Y. Xu, K. F. LaNoue, T. W. Gardner and S. W. Levison, Minocycline reduces proinflammatory cytokine expression, microglial activation,

and caspase-3 activation in a rodent model of diabetic retinopathy, *Diabetes*, 2005, **54**(5), 1559–1565.

35 D. Boche, V. H. Perry and J. A. Nicoll, Review: activation patterns of microglia and their identification in the human brain, *Neuropathol. Appl. Neurobiol.*, 2013, **39**(1), 3–18.

36 X. G. Luo and S. D. Chen, The changing phenotype of microglia from homeostasis to disease, *Transl. Neurodegener.*, 2012, **1**(1), 9.

37 H. R. Wong, J. D. Finder, K. Wasserloos, C. J. Lowenstein, D. A. Geller, T. R. Billiar, B. R. Pitt and P. Davies, Transcriptional regulation of iNOS by IL-1 beta in cultured rat pulmonary artery smooth muscle cells, *Am. J. Physiol.*, 1996, **271**(1 Pt 1), L166–L171.

38 R. Ferreira, T. Santos, L. Cortes, S. Cochaud, F. Agasse, A. P. Silva, S. Xapelli and J. O. Malva, Neuropeptide Y inhibits interleukin-1 beta-induced microglia motility, *J. Neurochem.*, 2012, **120**(1), 93–105.

39 E. Ruoslahti, RGD and other recognition sequences for integrins, *Annu. Rev. Cell Dev. Biol.*, 1996, **12**, 697–715.

40 E. F. Plow, T. A. Haas, L. Zhang, J. Loftus and J. W. Smith, Ligand binding to integrins, *J. Biol. Chem.*, 2000, **275**(29), 21785–21788.

41 B. T. MacDonald, K. Tamai and X. He, Wnt/beta-catenin signaling: components, mechanisms, and diseases, *Dev. Cell*, 2009, **17**(1), 9–26.

42 C. P. Pereira, E. B. Bachli and G. Schoedon, The wnt pathway: a macrophage effector molecule that triggers inflammation, *Curr. Atheroscler. Rep.*, 2009, **11**(3), 236–242.

43 C. Halleskog and G. Schulte, Pertussis toxin-sensitive heterotrimeric G proteins mediate WNT/beta-catenin and WNT/ERK1/2 signaling in mouse primary microglia stimulated with purified WNT-3A, *Cell Signal*, 2012, **25**(4), 822–828.

44 J. C. Gross, V. Chaudhary, K. Bartscherer and M. Boutros, Active Wnt proteins are secreted on exosomes, *Nat. Cell Biol.*, 2012, **14**(10), 1036–1045.

45 C. Hooper, R. Sainz-Fuertes, S. Lynham, A. Hye, R. Killick, A. Warley, C. Bolondi, J. Pocock and S. Lovestone, Wnt3a induces exosome secretion from primary cultured rat microglia, *BMC Neurosci.*, 2012, **13**, 144.

46 T. P. Kunzler, T. Drobek, M. Schuler and N. D. Spencer, Systematic study of osteoblast and fibroblast response to roughness by means of surface-morphology gradients, *Biomaterials*, 2007, **28**(13), 2175–2182.

47 K. Kubo, W. Att, M. Yamada, K. Ohmi, N. Tsukimura, T. Suzuki, H. Maeda and T. Ogawa, Microtopography of titanium suppresses osteoblastic differentiation but enhances chondroblastic differentiation of rat femoral periosteum-derived cells, *J. Biomed. Mater. Res., Part A*, 2008, **87**(2), 380–391.

48 F. Zheng, X. Zhou, C. Moon and H. Wang, Regulation of brain-derived neurotrophic factor expression in neurons, *Int. J. Physiol., Pathophysiol. Pharmacol.*, 2012, **4**(4), 188–200.

49 K. Wegner, P. Piseri, H. Vahedi Tafreshi and P. Milani, Cluster beam deposition: a tool for nanoscale science and technology, *J. Phys. D: Appl. Phys.*, 2006, **39**, R439–R459.

50 H. V. Tafreshi, P. Piseri, G. Benedek and P. Milani, The role of gas dynamics in operation conditions of a pulsed microplasma cluster source for nanostructured thin films deposition, *J. Nanosci. Nanotechnol.*, 2006, **6**(4), 1140–1149.

51 P. Piseri, H. Vahedi Tafreshi and P. Milani, Manipulation of nanoparticles in supersonic beams for the production of nanostructured materials, *Curr. Opin. Solid State Mater. Sci.*, 2004, **8**(3–4), 195–202.

52 E. Barborini, I. N. Kholmanov, A. M. Conti, P. Piseri, S. Vinati, P. Milani and C. Ducati, Supersonic cluster beam deposition of nanostructured titania, *Eur. Phys. J. D*, 2003, **24**(1–3), 277–282.

